

## NON-STATIONARY HEATING OF LOW-POWER INDUCTION MOTOR UNDER CONTINUED OVERLOAD

Andris Sniders, Alexey Gedzur

Latvia University of Agriculture

andris.sniders@llu.lv, aleksejs.gedzurs@inbox.lv

**Abstract.** The paper discusses transient heating processes and the response of a low-power induction motor to permanent constant load, overload and a locked rotor under a standard electrical supply system (380V, 50 Hz) for cold initial conditions and constant ambient temperature. The experimental investigations are performed on a 1.1 kW totally enclosed fan-cooled three-phase induction motor. The transient temperatures are measured in 6 points of the stator end windings and in 2 points of the motor casing using thermocouples, current sensors and loggers for data processing and archiving. The resistive stator losses for single-phase are calculated using the stator windings equivalent parameters, considering the dynamic change of the stator current and the windings resistance from temperature. The experimental tests and analytical calculations show that the stator windings heating curves obey the first order non-stationary thermal process with time dependent thermal capacity and heat dissipation factor, as the functions of the motor part temperature. Analyses of the study results show, that an adaptive self-tuning virtual model of the induction motor thermal process should be composed for adequate programming of the processor-based motor protective devices to improve their operation quality.

**Key words:** induction motor, current, losses, heating temperature, continued overload, thermal model.

### Introduction

Low voltage induction motors (400 V, 50 Hz) have got large applications in industry and agriculture, consuming the majority of the total electrical energy consumption in the world. They are available in a wide choice, as from several tens watts up to several hundreds kilowatts. Typical induction motor (IM) applications in rural industry include pumps, fans, compressors, mills, saw machines, cranes, conveyors, crushers, etc. The statistics have shown that despite the IM high reliability and simplicity of construction, the annual motor failure rate is conservatively estimated at 3-5 % per year, and in extreme cases, up to 12 % [1]. IM failures cause essential direct and technological losses involving the motor replacement and repair, as well as interruption of the production process.

IM failures may be classified as follows: 1) electrical related failures ~35 %; 2) mechanical related failures ~31 %; 3) environmental impact and other reasons related failures ~34 % [1]. Analyses of the IM failure reasons show that many of them are caused by prolonged heating of the different parts involved in IM operation. That is why an accurate tracking of the IM thermal status and adequate response of the protection system to thermal overloads is very important. Modern trends in electric motor construction are to make IM more compact and efficient. At the same time the new IM are more sensitive to mechanical and electrical overloads. On the other hand, overestimation of the thermal state of the induction motor can cause undesirable IM stoppage and useless interruption of the production process. Therefore, it is very important to predict the thermal condition of the induction motor and to develop a desirable accurate and flexible thermal model of IM operation under prolonged overload.

A detailed description of experimental and analytical research methods and results of the transient heating of IM parts and thermal modelling is given in [2]. If the thermal model is used in the IM design process, a fairly complex model is necessary, based on the numerical finite element method. If the thermal model is used for determining the heating of the existing IM parts, a simpler model can be used, often referred to as the thermal network model [2].

The most sensitive part of IM to thermal overloads is stator windings. The main limiting factor of IM continuously loading is the stator winding temperature. Exceeding the temperature limit, results in acceleration of the oxidation process in the insulation materials what eventually leads to IM damage. Commonly for the heating process of the IM stator windings the first-order thermal model with constant parameters [3] or two level variable parameters, different for initial and for final periods have been used [1]. For instance, the thermal and electrical parameters of IM vary continuously during all heating transient process. Application of soft starters and frequency converters increase the losses due to higher harmonics and cause more intensive heating of the IM stator windings and other parts [4; 5].

The main tasks of this work are to get experimental characteristics and thermal parameters of the IM stator winding heating process for cold initial condition and prolonged rated load, overload and locked rotor.

### Research object and methods

The thermal research object is a three phase induction motor: 4AX80A4Y3; 220/380 V; 4.9/2.8 A; IP44; ins.cl. [B],  $m = 14.5$  kg;  $P = 1.1$  kW;  $n = 1400$  min<sup>-1</sup>;  $s = 0.067$ ;  $\eta = 0.75$ ;  $\cos\phi = 0.81$ . The stator circuit parameters: resistance  $R_{\theta a} = 7.9$   $\Omega$  and impedance  $Z_s = 17.3$   $\Omega$  at ambient temperature  $\theta_a = 24$  °C are obtained by measuring. Reactance is calculated from  $X_s = (Z_s^2 - R_{\theta a}^2)^{0.5} = 15.4$   $\Omega$ . A direct current generator (P-22Y4, 220 V, 5.9 A,  $P = 1$  kW,  $n = 1500$  min<sup>-1</sup>) and a lamp rheostat for IM loading is used.

The block diagram of the test bench set-up for conducting the experimental tests is shown in Figure 1. The test bench is fitted with adequate laboratory measuring equipment – voltmeters (V), ammeters (A) and watt meters (W) for monitoring of three phase current, voltage and power. For precise measuring of IM stator casing (frame) and winding temperature, eight miniature thermocouples BK-50 (air probe – SE000) are installed. All thermocouples are connected to a data logger TC-08 with built in cold junction compensation (PICOLOG software, Windows driver, accuracy of temperature reading -  $\pm 0.5$  °C). The stator casing surface temperatures are measured in two points by thermocouples  $T_4$  and  $T_5$ . They are mounted at the casing shaft side and fan side (Fig. 1). The stator winding temperatures are measured for each phase (A, B, C) by six thermocouples attached to the end windings. Three thermocouples ( $T_1, T_2, T_3$ ) are placed at the shaft (drive) side and the other three ( $T_6, T_7, T_8$ ) – at the fan side. To get a good thermal contact, the thermocouples are inserted into natural gaps in the end windings and bonded by thermal bandage. For precise measuring of IM stator current during all transient heating process the current sensors – current clamps – 3XTA011AC and the data logger – EL005 (accuracy  $\pm 1$  %) are installed.

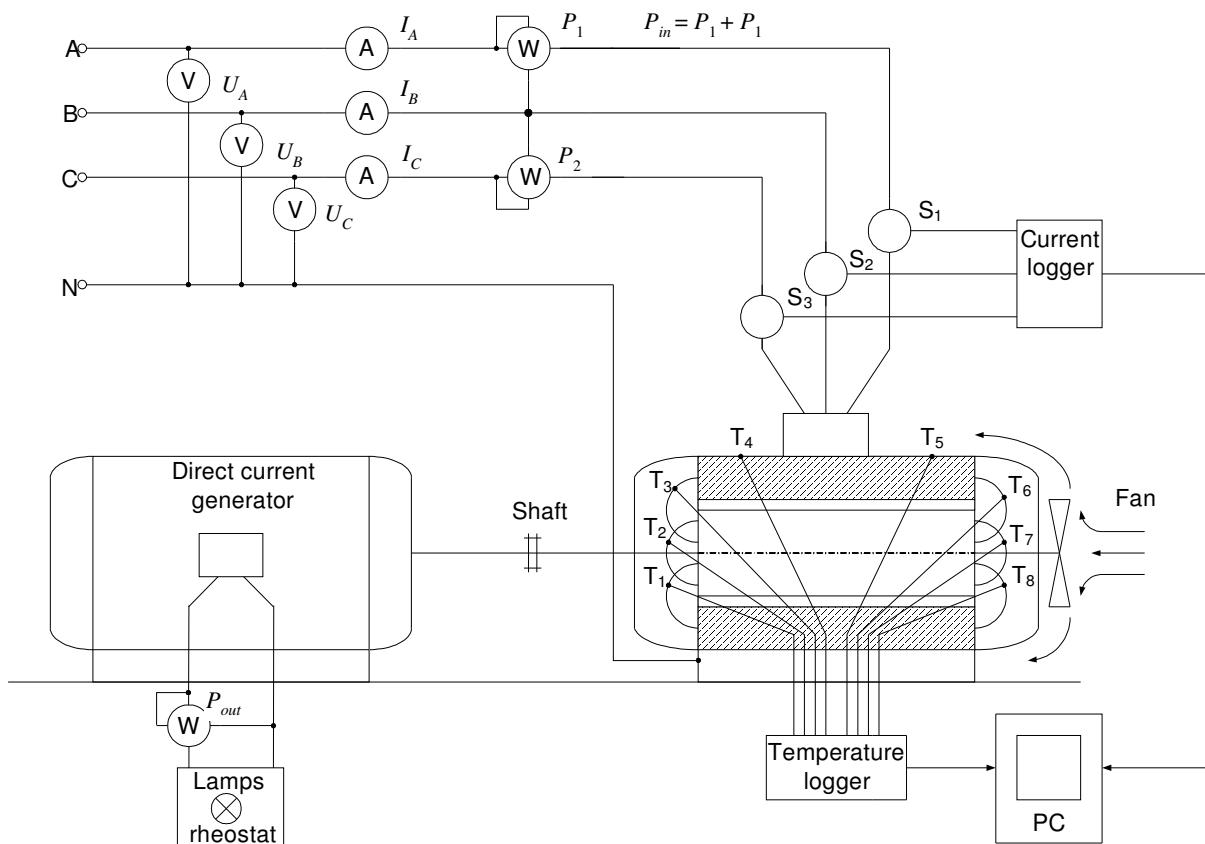


Fig. 1. Test bench set-up for induction motor heating experimental research:

$T_1, T_2, T_3$ , – thermocouples (end windings – shaft side);  $T_4, T_5$  – thermocouple (casing – shaft side, fan side);  $T_6, T_7, T_8$ , – thermocouples (end windings – fan side);  $S_1, S_2, S_3$  – current sensors

All heating tests are made for cold initial conditions – initial temperature of IM all parts is equal to ambient temperature ( $\theta_0 = \theta_a$ ). Supply voltage and frequency are traditional and uniform with the rated values (380 V, 50 Hz) in all phases. The winding and casing temperatures transient rise test series are run for three modes of IM operation: 1) rated load; 2) overload; 3) locked rotor (standstill). IM load is determined by a coefficient in relation to the stator current –  $k_i = I_s/I_r$ , where  $I_s$  – actual stator current, A;  $I_r$  – rated stator current, A. The results of IM heating experimental research are shown in Figures 2., 3., 4.

**Results and discussion**

**1. IM heating response to permanent mechanical load under cold initial conditions**

Figure 2 shows the IM thermal response to permanent rated load. The initial temperature of IM all parts equal to ambient temperature  $\theta_0 = \theta_a = 26\text{ }^\circ\text{C}$ . The loading generator is charged to the lamp rheostat according to the IM approximate rated current  $I_0 = 2.67\text{ A}$ . The stator winding temperature rise causes the stator current reduction from the beginning value 2.67 A at  $26\text{ }^\circ\text{C}$  to the end value 2.52 A at  $85\text{ }^\circ\text{C}$  because of windings resistance growth. Relative stator current  $k_i = I_s/I_r = 2.67/2.8 = 0.95$ .

The shaft side end windings steady-state temperature  $\theta_s$  is up to  $6\text{ }^\circ\text{C}$  higher than the fan-side temperature because of the different heat dissipation value  $H\text{ (W}\cdot\text{ }^\circ\text{C}^{-1})$ . The fan side cooling conditions are better, therefore the  $H$  value is higher and the end windings temperature is lower. The frame heating characteristics demonstrate an essential role of ventilation on the cooling efficiency. The fan side steady-state temperature  $\theta_{cf} = 37\text{ }^\circ\text{C}$  is 40 % lower than the shaft side one –  $\theta_c = 52\text{ }^\circ\text{C}$ .

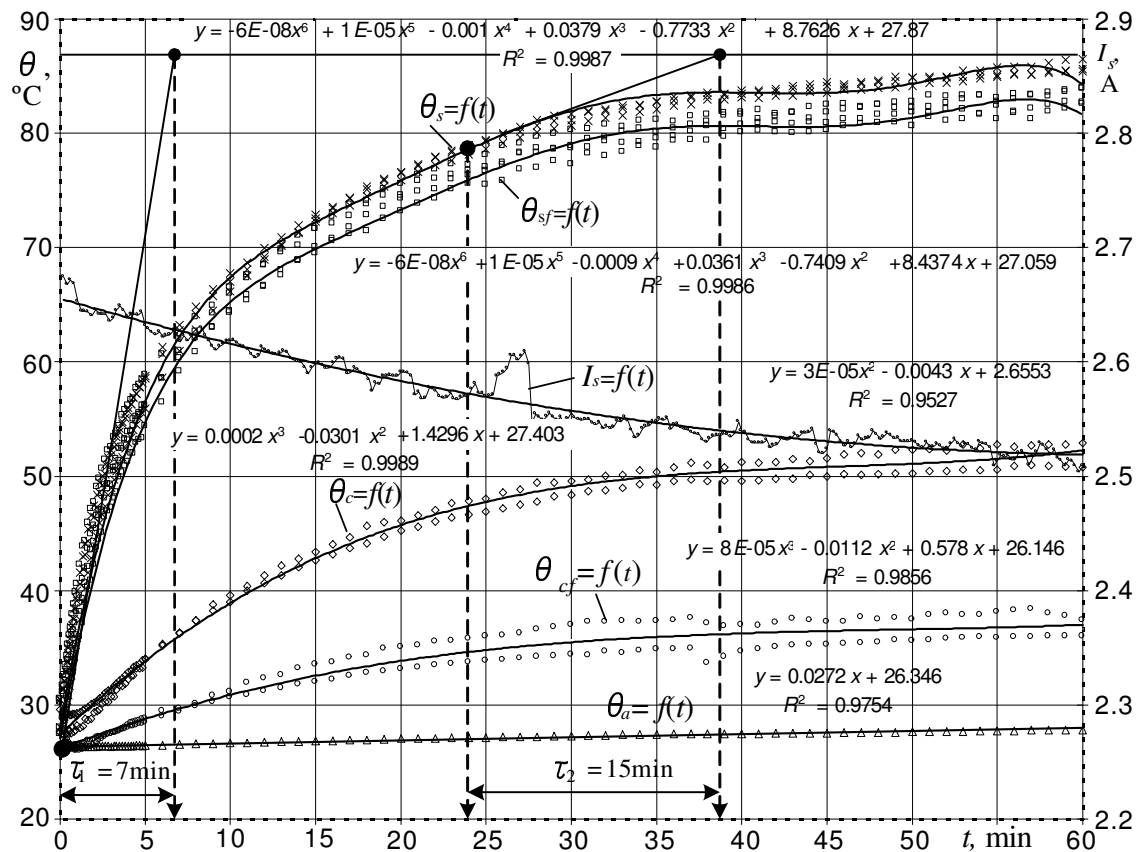


Fig. 2. Response of induction motor part temperature to permanent rated load for cold initial conditions:  $\theta_s(t)$ , – temperature of stator end windings – shaft side, °C;  $\theta_{sf}$ , – temperature of stator end windings – fan side, °C;  $\theta_c(t)$ , – temperature of casing – shaft side, °C;  $\theta_{cf}(t)$ , – temperature of casing – fan side, °C;  $\theta_a(t)$ , – ambient temperature, °C;  $I_s(t)$  – stator current, A;  $\tau_1$ ,  $\tau_2$  – thermal time constants

Figure 3 shows the IM thermal response to permanent overload by the stator current:  $k_i = I_s/I_r = 3.18/2.8 = 1.14$  (14 %). The initial temperature of IM all parts is equal to ambient temperature  $24\text{ }^\circ\text{C}$ . The loading generator is charged according to the IM overload initial current

$I_0 = 3.18$  A. The stator winding temperature rise causes the stator winding resistance growth and current reduction from the beginning value 3.18 A at 24 °C to the end value 2.95 A at 110 °C. Under overload the ventilation effect on temperature difference at the shaft side and fan side is greater. The end winding shaft side steady-state temperature is up to 10 °C higher than the fan-side temperature but the difference of the casing surface temperatures is up to 50 %. Under higher overloads the role of ventilation on the cooling efficiency of the IM windings and casing increases. It is a problem for the high slip induction motors. Interpolations of the IM heating tests testify that the stator windings thermal model is non-stationary with temperature dependent parameters. Even the 6<sup>th</sup> order polynomial regression dissatisfies the needed dynamic accuracy.

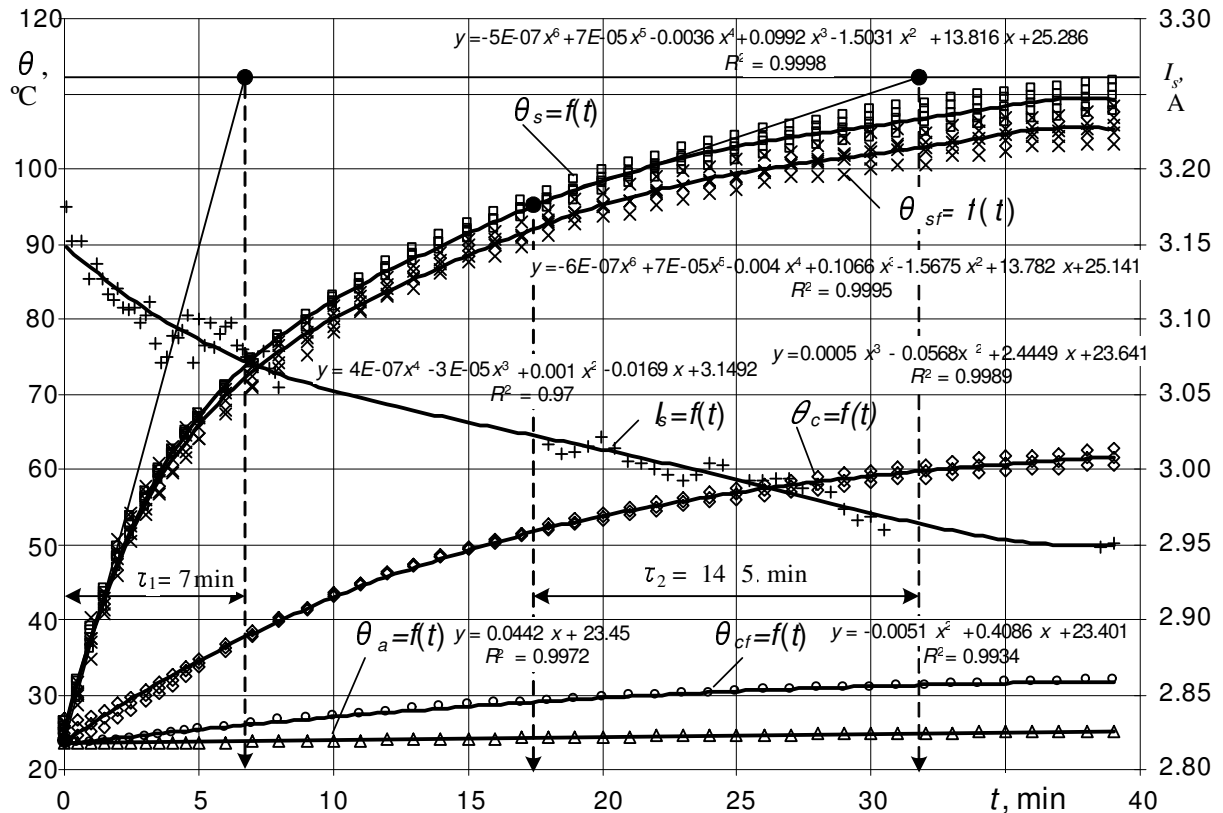


Fig. 3. Response of induction motor part temperature to permanent overload for cold initial conditions:  $\theta_s(t)$ , – temperature of stator end windings – shaft side, °C;  $\theta_{sf}$ , – temperature of stator end windings – fan side, °C;  $\theta_c(t)$ , – temperature of casing – shaft side, °C;  $\theta_{cf}(t)$ , – temperature of casing – fan side, °C;  $\theta_a(t)$ , – ambient temperature, °C;  $I_s(t)$  – stator current, A;  $\tau_1, \tau_2$  – thermal time constants

The cooling efficiency of the IM stator windings depends on the heat dissipation factor  $H_w$ . If the power losses  $P_w$  and the corresponding steady state temperature  $\theta_s$  of the stator windings is determined by the experiment, the heat dissipation factor can be calculated:

$$H_w = \frac{I_s^2 \cdot R_0 \cdot (\alpha_c^{-1} + \theta_s)}{(\theta_s - \theta_0) \cdot (\alpha_c^{-1} + \theta_0)}, \quad (1)$$

- where  $I_s$  – stator current at given stator windings temperature, A;
- $\theta_s$  – steady-state temperature of stator windings, °C;
- $\theta_0 = \theta_a$  – initial temperature of stator windings, equal to ambient temperature  $\theta_a$ , °C;
- $R_0$  – resistance of stator windings at ambient temperature,  $\Omega$ .
- $\alpha_c = 4.26 \cdot 10^{-3} \text{ } ^\circ\text{C}^{-1}$  – resistance-temperature coefficient of the cooper.

Calculations according to expression (1) show that at rated load steady-state  $H_w = 1.04 \text{ W} \cdot ^\circ\text{C}^{-1}$ , but at overload 14 % it is higher –  $1.07 \text{ W} \cdot ^\circ\text{C}^{-1}$ , because of higher final temperature.

If the load torque exceeds the critical torque, the IM rotor stays at a standstill mode. Losses in the stator windings are maximal  $P_w = \max$ , the rotation speed  $n = 0$ , the fan is out of order and heat

dissipation from the winding area  $H_w = \min$ . The heating process is adiabatic and after transient time, caused by thermocouples reaction delay, temperature rises gradually with constant ramp  $v_\theta = 5 \text{ }^\circ\text{C}\cdot\text{s}^{-1}$  (Fig. 4). Temperature measuring steady state error  $\Delta \theta = v_\theta \cdot \tau = \theta_s - \theta_{sm} = 10 \text{ }^\circ\text{C}$ , where  $\tau = 2\text{ s}$  – thermocouples thermal time constant, s;  $\theta_s$  – actual temperature,  $^\circ\text{C}$ ;  $\theta_{sm}$  – measured temperature,  $^\circ\text{C}$ . The casing temperature  $\theta_c$  stays constant all period of the winding temperature rise from ambient temperature to the limit one –  $130 \text{ }^\circ\text{C}$  (insulation class B). That testifies an adiabatic character of the stator winding heating process under the rotor standstill mode. In this case the stator winding thermal model should be highly precise to provide the tripping of the protection device with appropriate accuracy. On the basis of the test results (Fig. 4) the stator winding transient temperature  $\theta_s(t)$  at locked rotor can be expressed by a simple mathematical model:

$$\theta_s(t) = \theta_0 + \frac{I_{lr}^2 \cdot R_{lr} \cdot t}{H_{lr} \cdot \tau_{lr}}, \tag{2}$$

where  $I_{lr} = 12.5 \text{ A}$  – average stator current at long-term locked rotor;  
 $R_{lr} = 9.2 \text{ } \Omega$  – average stator windings resistance at long-term locked rotor;  
 $H_{lr} = 0.54 \text{ W} \cdot \text{ }^\circ\text{C}^{-1}$  – average stator windings heat dissipation factor;  
 $\tau_{lr} = 15.1 \text{ min}$  – average stator winding thermal constant at long-term locked rotor.

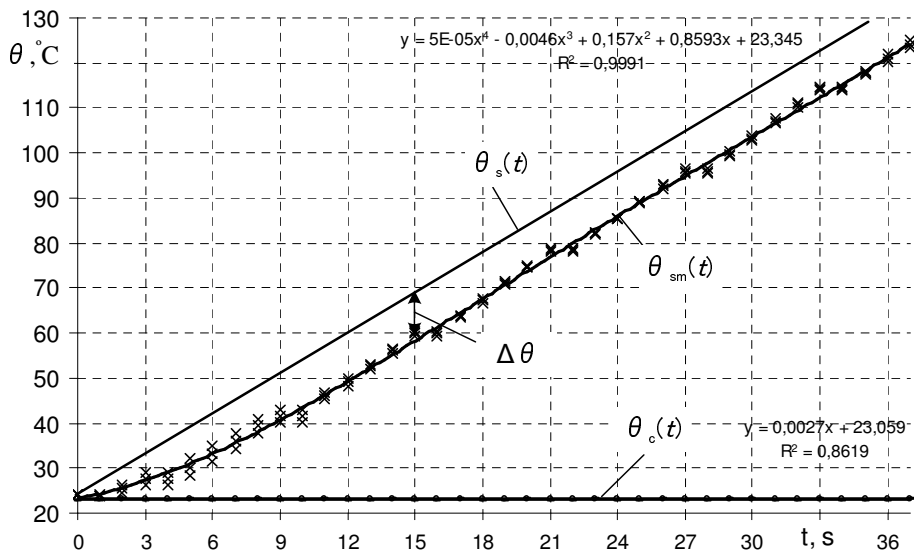


Fig. 4. Response of induction motor part temperature to locked rotor mode for cold initial conditions:  $\theta_s(t)$  – actual temperature of stator end windings – shaft side,  $^\circ\text{C}$ ;  $\theta_{sm}$ , – measured temperature of stator end windings – shaft side,  $^\circ\text{C}$ ;  $\theta_c(t)$ , – temperature of casing – shaft side,  $^\circ\text{C}$ ;  $\Delta\theta$  – measurement steady-state error of locked motor stator winding temperature,  $^\circ\text{C}$

**2. Thermal model of IM stator windings**

The steady-state performance of the IM stator winding heating temperature under load and overload can be described by the following equation:

$$\theta_s = \theta_0 + K(n, \theta_s) \cdot P_0 = \theta_0 + K(n, \theta_s) \cdot I_0^2 \cdot R_0, \tag{3}$$

where  $K(n, \theta_s)$  – variable sensitivity factor as a function of rotation speed and temperature,  $^\circ\text{C} \cdot \text{W}^{-1}$ ;  
 $P_0$  – single-phase initial power losses at ambient temperature, W;  
 $I_0$  – initial stator current at ambient temperature, A.

The measured single-phase resistance of the stator winding is  $R_0 = (7.9 \pm 0.05) \text{ } \Omega$ , if  $\theta_a = (22 \pm 2) \text{ }^\circ\text{C}$ .

The variable sensitivity factor  $K(\theta_s)$  changes during all transient heating process in accordance with the expression:

$$K(n, \theta_s) = \frac{(1+k_\rho) \cdot k_{\theta_s}}{(1+k_\rho \cdot k_{\theta_s}^2) \cdot H(n, \theta_s)} = \frac{[1 + (\frac{R_0}{X_s})^2] \cdot \frac{\alpha_c^{-1} + \theta_s}{\alpha_c^{-1} + \theta_0}}{[1 + (\frac{R_0}{X_s})^2 \cdot (\frac{\alpha_c^{-1} + \theta_s}{\alpha_c^{-1} + \theta_0})^2] \cdot H(n, \theta_s)}, \quad (4)$$

where  $k_\rho = (7.9/15.4)^2 = 0.26$  – square of the relation of initial resistance to reactance;  
 $k_{\theta_s}$  – resistance relative change in order of temperature;  
 $H(n, \theta_s)$  – heat dissipation factor as a function of rotation speed and temperature,  $W \cdot ^\circ C^{-1}$ ;  
 $n$  – IM rotation speed under variable load (rated value  $1400 \text{ min}^{-1}$ );  
 $X_s = 15.4 \Omega$  – single-phase stator windings reactance.

The heat dissipation factor changes substantially from the rotation speed and the temperature:

$$H(n, \theta_s) = [h_0 + \Delta h(n, \theta_s)] \cdot S, \quad (5)$$

where  $h_0$  – heat transfer coefficient at  $n = 0$  and  $\theta_s = \theta_0 = \theta_a$ ,  $W \cdot (m^2 \cdot ^\circ C)^{-1}$ ;  
 $\Delta h(n, \theta_s)$  – heat transfer coefficient rise as a function of  $n$  and temperature  
 $\theta_s$ ,  $W \cdot (m^2 \cdot ^\circ C)^{-1}$ ;  
 $n$  – IM rotation speed under variable load (rated value  $1400 \text{ min}^{-1}$ );  
 $S$  – dissipation heat surface area,  $m^2$ .

According to the investigations of Gunnar Kylander [2],  $h_0 = 6.5 \text{ W} \cdot (m^2 \cdot ^\circ C)^{-1}$ ,  $\Delta h = 5.25 \cdot u_r^{0.6}$  at indefinite temperature  $\theta_s$ , where  $u_r$  – rotor peripheral speed,  $m \cdot s^{-1}$ . The previous modeling of electrical thermal units [6] and analyses of heating characteristics (Fig. 2 – 4) allows making a conclusion that the model of the heat dissipation factor for the stator windings can be searched in the following form:

$$H(n, \theta_s) = \left\{ h_0 + e_n \left( \frac{n \cdot r}{9.55} \right)^a + e_\theta [(\theta_s - \theta_a) + b \cdot \sqrt{(\theta_s - \theta_a)}] \right\} \cdot S, \quad (6)$$

where  $e_n, e_\theta, a, b$  – empirical coefficients, obtained from the heating tests;  
 $r$  – IM rotor peripheral radius, m.

The stator winding thermal time constant depends on the thermal capacity  $C$  ( $J \cdot ^\circ C^{-1}$ ) of the IM parts, involved in heat dissipation from the windings, and on the heat dissipation factor  $H$  ( $W \cdot ^\circ C^{-1}$ ):

$$\tau_w = \frac{C[\theta_s(t)]}{H[n, \theta_s(t)]}. \quad (7)$$

The graphical analyses, using the tangent method, shows that the stator winding thermal time constant  $\tau_w$  changes all over the transient heating process (Fig. 1, Fig. 2). Initially, it has minimal value ( $\tau_w = \tau_1$ ), because of minimal mass involved in the heat transfer process ( $C = \text{min}$ ) and a higher sensitivity factor  $K$  (4), caused by a lower heat dissipation factor ( $H = \text{min}$ ). All is vice versa at the end of the temperature rise – the final time constant is substantially higher than the initial one ( $\tau_2 \gg \tau_1$ ). Therefore, according to the stator winding heating process, an induction motor is a non-stationary object with time dependent factors of thermal delay and heating sensitivity.

## Conclusions

1. The most sensitive part of the induction motor to thermal overload is the stator windings. The choice of the IM size and modification, as well as the choice, setup and programming of the motor protection device largely depends on the stator winding heating dynamics, what in its turn is determined by the motor parameters, motor mechanical load and environment conditions.
2. Investigation of the induction motor (4AX80A4Y3: 220/380 V, 4.9/2.8 A, 1.1 kW,  $1400 \text{ min}^{-1}$ ) transient heating shows that the initial ramp of the stator winding temperature rise is substantially higher, because of minimal thermal time constant ( $\tau_1 \approx 7 \text{ min}$ ) in comparison with that at the end of the process ( $\tau_2 \approx 15 \text{ min}$ ) when temperature becomes steady.

3. According to the stator winding heating process, an induction motor is a non-stationary thermal object with a time dependent continuously increasing thermal delay factor and falling sensitivity factor during all the transient process of temperature rise.

### References

1. Venkataraman B., Godsey B., Premerlani W., Shulman E.etc. Fundamentals of a Motor Thermal Model and its Applications in Motor Protection. In: Proceedings of 58<sup>th</sup> Annual Conference “Protective Relay Engineers”, Black & Veatch Corporation, Kansas City, USA, 2005, pp. 127 – 144.
2. Kylander G. Thermal Modelling of Small Cage Induction Motors: Technical Report No. 265, Goteborg, Sweden, Chalmers University of Technology, 1995. – 113 p.
3. Zocholl S.E., Benmouyal G. Using Thermal Limit Curves to Define Thermal Models of Induction Motors. Schweitzer Engineering Laboratories, Pennsylvania (USA), Quebec (Canada), Printed in USA, 2001. – 14 p.
4. Mukhopadhyay S.C. Prediction of Thermal Condition of Cage-Rotor Induction Motors under Non – Standard Supply Systems. International Journal on Smart Sensing and Intelligent Systems, Vol.2, No. 3, 2009, pp. 381 – 395.
5. Solveson M. G., Mirafzal B., Demerdash N. A. O. Soft-Started Induction Motor Modeling and Heating Issues for Different Starting Profiles Using a Flux Linkage ABC Frame of Reference. IEEE Transactions on Industry Applications, Vol. 42, No. 4, 2006, pp. 973 – 983.
6. Sniders. A. Adaptive Self-Tuning up Model for Non-Stationary Process Simulation. In: Proceedings of the 9<sup>th</sup> International Scientific Conference “Engineering for Rural Development”. – Jelgava: LUA, 2010, pp. 192 – 199.